Gazi University Journal of Science
GU J Sci
28(2):275-283 (2015)

Dynamic Modeling and Experimental Validation of a Dual-Stator PMSG for Low Speed Applications

Ali Reza DEHGHANZADEH [1,♠], Vahid BEHJAT [2]

[1,2]*Department of Electrical Engineering, Faculty of Engineering, Azarbaijan Shahid Madani University, Tabriz, Iran*

Received: 26/09/2014 Revised: 21/12/2014 Accepted: 21/02/2015

ABSTRACT

This research work develops dynamic model and experimental validation of a dual-star PMSG. A technique of transforming the two stator winding sets to the two winding couples on the d-q axes of the rotor reference frame is utilized in dynamic modeling issue. The implemented technique results in simplifying of analyzing of the machine. To validate the developed dynamic model of the machine, the same PMSG used with the dynamic modeling is constructed and used in an experimental set-up. The simulation and experimental results prove the proper performance of the developed model of the machine and its experimental design.

Key Words: permanent magnet synchronous generator, dual-star, dynamic modeling.

1. INTRODUCTION

In recent years, the distributed generation (DG) has attracted more attention due to system losses mitigation, reduction of voltage drop, system reliability improvement and etc. Growing environmental concerns and attempts to reduce dependency on fossil fuel resources are bringing renewable energy sources to the mainstream of the electrical power sector [1]. Wind power is one of the renewable energies that received more attention due to its clean and economical characteristics, and it is predicted that by 2020 up to 12% of the words electricity will be supplied by wind power [2-3].

The existing wind power generation systems can be categorized into three main types: 1) fixed-speed squirrel-cage induction generators; 2) variable-speed doubly fed induction generators (DFIG); and 3) variable-speed synchronous generators, which are either a wound rotor synchronous generator or a permanent-magnet synchronous generator (PMSG). Today variable speed wind turbines have become more common than traditional fixed speed turbines because of the more efficient energy production, improved power quality and improved dynamic performance during grid disturbances [4, 5]. In addition, they can reduce mechanical stresses respect to fixed speed wind turbines [6-7]. In recent years, the PMSGs meet increasing application in wind turbines industry owing to the development of permanent magnet (PM) materials. The PMSGs are designed in multiple poles due to using PM, which results in elimination of the gear box. Compared to DFIG, a direct drive PMSG based wind turbine reduces system failure rate due to absence of mechanical gearbox. Also, the PMSGs provide high power generation efficiency because of rotor losses reduction [8-11].

From the windings design point of view, the PMSGs can be designed in two configuration forms: one and dual-star. The dual star PMSGs consist of two three phase winding sets that spatially displaced 30 electrical degrees. The dual-star PMSG offers several advantages in terms of: reduction of DC link current and voltage ripple, lower torque pulsation and better fault tolerance. Furthermore, the series-parallel connection of the rectified outputs of two three phase groups can be favorable option for variable speed wind turbine application in view of power electronic converters design [12-15].

A literature survey proves that there are limited research efforts [12-15] dealing with analysis and modeling of dual-star PMSGs. Ref. [12] deals with modeling and simulation about dual-star PMSG and there is no experimental design and experimental test validation. Ref. [13] deals with determining of machine inductance

♠Correspondingauthor, e-mail: s.dehghanzadeh@azaruniv.ac.ir, behjat@azaruniv.edu

parameters based finite element modeling (FEM) and simulation of dual-star PMSG model. Ref. [14] and [15] describe the application of dual-star PMSG for wind turbine based diode rectifiers.

The authors are involved in this study in extending the previous studies for modeling of the dual-star PMSG by developing a detailed model of the machine and its experimental validation. To this aim, the same PMSG used with the dynamic modeling is constructed and used in an experimental set-up. The dynamic modeling and experimental test are provided for a dual-star PMSG with rated electrical power of 300 (W), rated voltage of 150 (V) and 6 numbers of poles. The diode rectifiers are utilized in the output of studied dual-star PMSG in order to evaluate the proposed topology specifications. The rectified voltage and current of dual-star PMSG are comprised with single winding PMSG to provide the advantages of dual-star PMSG. Besides to, in this paper the agreement of the simulation results with experimental outputs and linear behavior of the proposed topology are evaluated.

The paper is organized as follows: Section 2 describes the details of the dynamic modeling of the dual-star PMSG. Section 3, starts with a brief description addressing the characteristics of the tested PMSG and then describes the simulation results of the machine. The construction details of the same machine used with the dynamic modeling and experimental tests which were conducted in laboratory on this machine for validating the developed dynamic model are described in Section 4. Discussion of the results and implications for future researches are also given in this section. Finally, conclusions will be given in the last section.

2. DUAL-STAR PMSG MODELLING

The topology of the dual-star PMSG is similar to the conventional PMSGs except for the stator windings and the number of diode rectifiers. The PMSG of the system has two sets of three-phase stator windings (stator1 and stator2) with a phase shift angle of 30 electrical degrees and it makes to reduction of rectified voltage and current ripple. As a result, the harmonics produced by diode rectifiers are decreased [12-15].

Fig. 1 shows the winding arrangement of the studied dual-star PMSG. There are two sets of three phases of windings on the stator side, which are galvanic ally isolated and shifted by 2α electrical degrees.

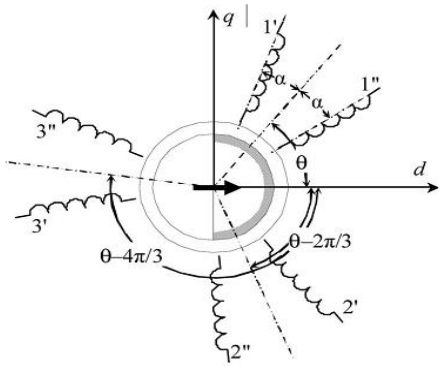

Fig. 1. Stator winding arrangement of dual-stator PMSG.

With negligible saturation effects, the following equalities can be expressed for armature inductances:

$$L_{1'1'} = L_{2'2'} = L_{3'3'} = L_{1''1''} = L_{2''2''} = L_{3''3''} = L_S \quad (1)$$

$$M_{1'2'} = M_{2'3'} = M_{3'1'} = M_{1''2''} = M_{2''3''} = M_{3''1''} = M_S \quad (2)$$

$$M_{1'1''} = M_{2'2''} = M_{3'3''} = M_a \quad (3)$$

$$M_{1'2''} = M_{2'3''} = M_{3'1''} = M_b \quad (4)$$

$$M_{1'3''} = M_{2'1''} = M_{3'2''} = M_c \quad (5)$$

Let $\delta = \theta \pm \alpha$ be the angular displacement of the axis of the reference stator winding ($1'$ or $1''$) with respect to the d-axis and $\lambda_{fs}(\delta)$ be the no load flux linkage of PMs. The PMs can be modeled with equivalent rotor winding supplied by a constant current I_f, where $M_{fs}(\delta) = \lambda_{fs}(\delta) / I_f$ is the mutual inductance with the stator winding. As depicted in Fig. 2, by transforming the two stator winding sets to the two winding couples on the d-q axes of the rotor reference frame, the voltage equation of the windings can be written as:

$$E_{0,d'q'} = V_{d'q'} + (R_{d'q'} + \omega J L_{d'q'} + L_{d'q'} P).I_{d'q'} \quad (6)$$

$$E_{0,d''q''} = V_{d''q'} + (R_{d''q''} + \omega J L_{d''q''} + L_{d''q''} P).I_{d''q''} \quad (7)$$

Where the parameters are defined as:

$$E_{0,d'q'} = -(p+\omega J).\Delta_{f'} \quad (8)$$

$$E_{0,d''q''} = -(p+\omega J).\Delta_{f''} \quad (9)$$

$$R_{d'q'} = R_{d''q''} = \begin{bmatrix} R_S & 0 \\ 0 & R_S \end{bmatrix} \quad (10)$$

$$\begin{aligned} \Delta_{f'} &= M_{f'} I_{f'} \\ \Delta_{f''} &= M_{f''} I_{f''} \end{aligned} \quad (11)$$

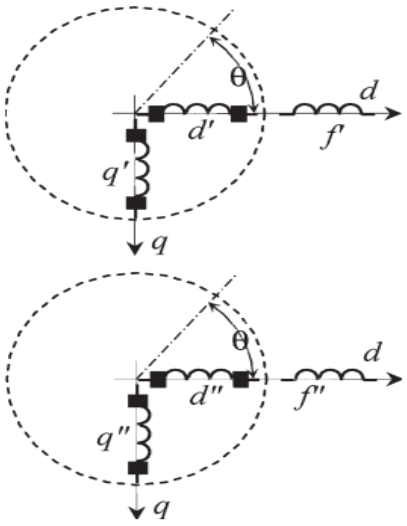

Fig. 2. Transformed windings decoupled with respect to each other.

Considering to equations (6), (7) the following complex variables are defined as:

$$e_0' = E_{0,d'} + jE_{0,q'} \quad (12)$$

$$e_0'' = E_{0,d''} + jE_{0,q''} \quad (13)$$

$$V_0' = V_{d'} + jV_{q'} \quad (14)$$

$$V_0'' = V_{d''} + jV_{q''} \quad (15)$$

$$i' = i_{d'} + ji_{q'} \quad (16)$$

$$i'' = i_{d''} + ji_{q''} \quad (17)$$

According to (12)-(17), the matrix equations (6) and (7) can be converted into the two scalar complex equations as:

$$e_0' = V' + (R_S + j\omega L' + L' p)i' \quad (18)$$

$$e_0'' = V'' + (R_S + j\omega L'' + L'' p)i'' \quad (19)$$

Where L' and L'' are equal to:

$$L' = L_S - M_S + \sqrt{M_a^2 + M_b^2 + M_c^2 - M_a M_b - M_b M_c - M_c M_a} \quad (20)$$

$$L'' = L_S - M_S - \sqrt{M_a^2 + M_b^2 + M_c^2 - M_a M_b - M_b M_c - M_c M_a} \quad (21)$$

For completing the dual-star PMSG modeling, it is necessary to convert the i' and i'' of the complex quantities in to the currents of actual windings. The matrix $T(\theta)$, which is defined as (22), and its conjugate transpose $(T^*(\theta))$ can be applied to convert the voltages and currents of the actual windings to the complex quantities and vice versa.

$$T(\theta) = \frac{1}{\sqrt{3}} \begin{bmatrix} e^{-j\alpha\bar{c}} & e^{j\alpha\bar{c}} \\ -je^{-j\alpha\bar{c}} & je^{-j\alpha\bar{c}} \end{bmatrix} \quad ,\bar{c} = e^{-j\theta} \begin{bmatrix} 1 & e^{j\frac{2\pi}{3}} & e^{j\frac{4\pi}{3}} \end{bmatrix} \quad (22)$$

The winding sets of the considered dual-star PMSG in this study are displaced 30 electrical degree which means that $2\alpha = \frac{\pi}{6}$. Fig. 3 shows the schematic block diagram of the dual-star PMSG dynamic modeling.

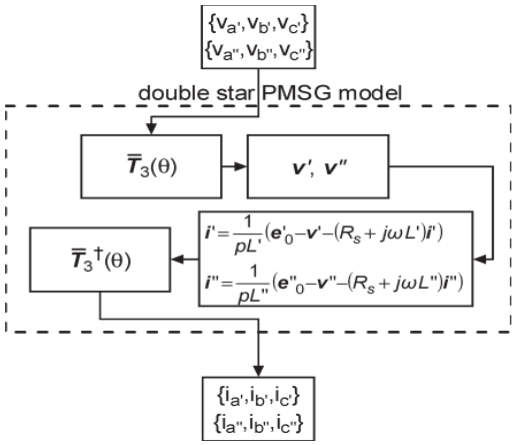

Fig. 3. Schematic diagram of the dual star PMSG dynamic modeling.

3. SIMULATION RESULTS

In this section, the simulation is provided for a dual-star PMSG based on the introduced dynamic modeling in section II. The simulated dual-star PMSG parameters are listed in Table I according to laboratory prototype as introduced in section IV. The simulation is carried out in the low rotor speeds about 210 (R.P.M). The output rectifiers of two winding sets are series connected and supply a constant current for resistive load (80Ω) as shown schematically in Fig. 4. Fig. 5(a) shows the phase currents of two winding sets of the simulated generator. It can be seen from the Fig. 5(a) that the phase currents of two winding sets have the same amplitude and 30 electrical degrees phase shift to each other. The rectified output voltage of one winding is shown in Fig. 5(b). As shown, the rectified output voltage of singular rectifier has 6 ripples in duration of one period (T=95.23 ms) and the DC voltage level is approximately 115 v. Fig. 5(c) presents the load DC rectified voltage in series connected of two rectifiers. The final output DC voltage has 12 ripples during one period. The ripples amplitude is decreased as compared to one singular rectifier output.

TABLE I. design parameters of the proposed machine.

Parameters	**Value**
Electrical power (w)	300
Rotor speed (R.P.M)	600
Rated voltage	150
Number of poles	6
N_{coil}	250
$N_{s,phase}$	500
Number of coils	12
Number of phases	6
Permanent Magnet Residual Flux Density	1.20 (T)

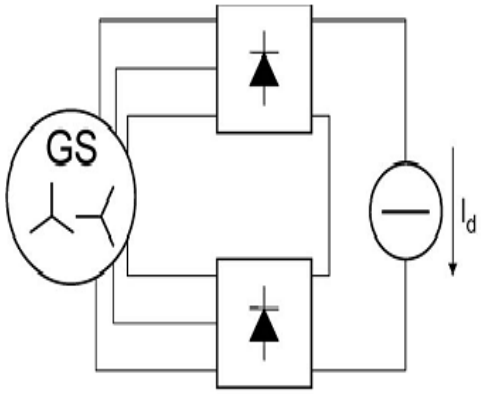

Fig. 4. Dual-star PMSG supplying a resistive load by two series connected rectifiers.

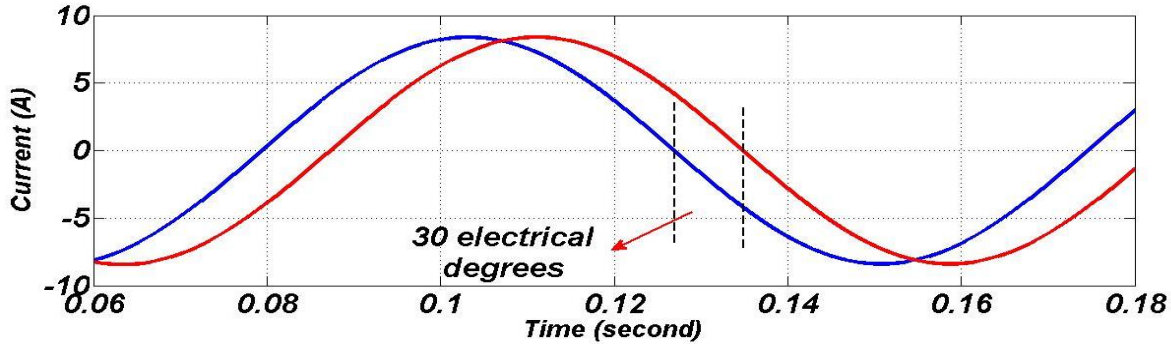

(a)

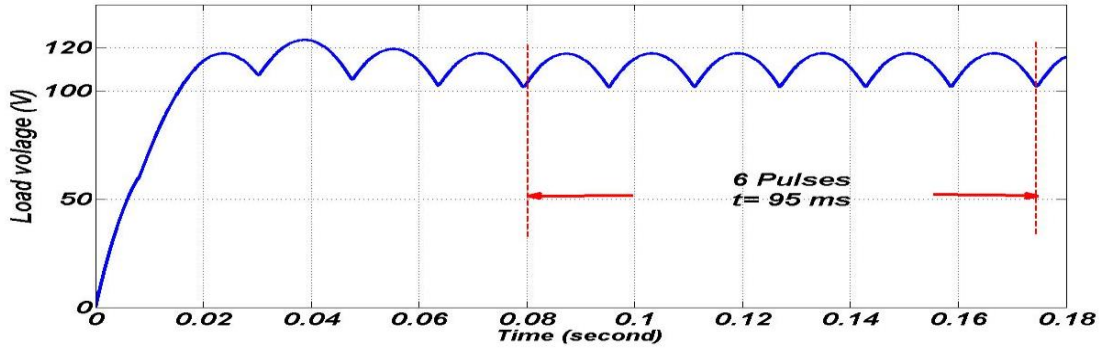

(b)

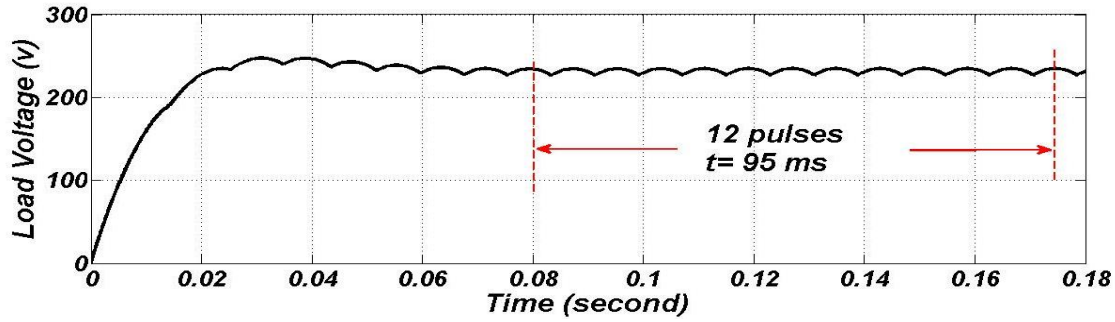

(c)

Fig. 5. Simulation results, (a) similar phase current of two winding sets, (b) rectified output voltage of singular rectifier, (c) load voltage in dual-star PMSG.

4. EXPERIMENTAL RESULTS

According to the main specifications and dimensions given in Table I and II, a prototype dual-star PMSG has been constructed and tested in order to demonstrate the possibility of the experimental test of proposed solution.

TABLE II. geometric parameters of the proposed machine.

parameter	Value(mm)
Inner radius of stator	77.5
Outer radius of stator	107.5
Inner radius of rotor	15
Outer radius of rotor	65
Air gap	4.5
Thickness	10
Inner radius of magnet	45
Outer radius of magnet	65

In order to validate the developed dynamic model in the previous section, the same machine used with the dynamic modeling was constructed in the laboratory and used in an experimental set-up to make measurements and conduct tests. Figs. 6(a) and (b) illustrate the detailed rotor structure and the winding coils of the machine stator respectively. The completed generator and the experimental setup which were used for conducting the tests are shown on the laboratory test bench in Fig. 6(c). Both stator windings are connected electrically in star connection. The machine is driven by an induction motor fed by a frequency converter and loaded with a resistive load.

(a)

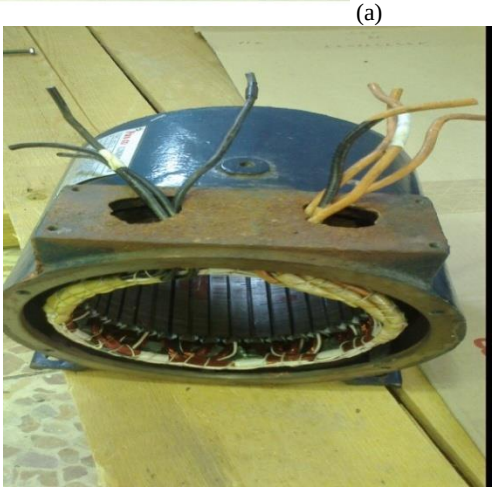

(b)

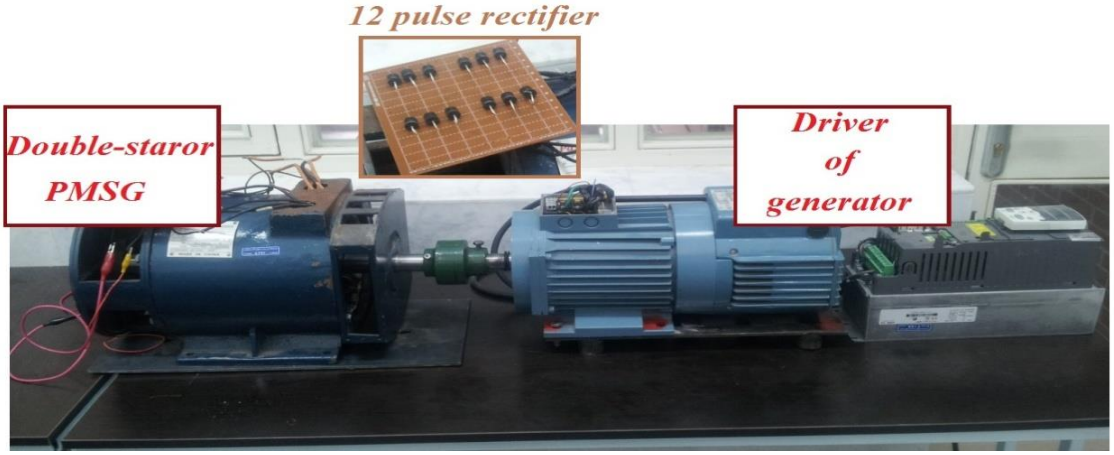

(c)

Fig. 6. (a) Detailed structure of the rotor, (b) Winding coils of the stator, (c) Experimental setup including the tested machine.

Figs. 7(a) to 7(e) present the experimental results, including recorded waveforms of the terminal values as well as rectified voltage of the windings and DC voltage of the load side, when the generator was rotated and loaded with the values as they have been in the simulation tests. Fig. 7(a) depicts the phase voltages of two winding sets of the tested generator. The waveforms given in Fig. 7(a) are corresponding to the

simulation results which were shown previously in Fig. 5(a). In complete agreement with the simulated traces in Fig. 5(a), it can be clearly seen from the figures that the phase voltages of two winding sets have the same amplitude and 30 electrical degrees phase shift to each other. The rectified output voltage of one winding is shown in Fig. 7(b). As shown, the rectified output voltage of singular rectifier has 6 ripples in duration of one period (T=95.23 ms) and the DC voltage level is approximately 115 V. The waveforms given in Fig. 7(b) are corresponding to the simulation results which were shown previously in Fig. 5(b). In complete agreement with the simulated traces in Fig. 5(b), it can be seen from the figures that the ripples of load voltage have the same mount and amplitude.

Fig. 7(c) presents the load DC rectified voltage in series connected of two rectifiers. The final output DC voltage has 12 ripples during one period. The ripples amplitude is decreased as compared to one singular rectifier output. The DC voltage level is about 230 V. The waveforms given in Fig. 7(c) are corresponding to the simulation results which were shown previously in Fig. 5(c). In complete agreement with the simulated traces in Fig. 5(c), it can be seen from the figures that the ripples of load voltage have the same mount and amplitude in single winding form. The current waveform of one phase is shown in Fig. 7(d). Figs. 8(a) to 8(c) present the three phase voltage waveforms of one of the winding sets in different rotor speeds such as 300, 210 and 154 R.P.M to evaluate the liner function between rotor speed and generator output voltage. As shown in Fig. 8, the decreasing of rotor speed makes to reduction of winding voltage amplitude in the same rating.

Comparing the corresponding results obtained from simulation and real measurements on the machine in the laboratory proves the sensitivity and reliability of the developed dynamic model of the machine. It should be remarked that the small differences between the measured and simulated results observed in the figures, were caused by natural variation in the construction and measuring process and rather than by the developed model inaccuracies. Future work ought to focus on the connection of dual-star PMSGs to the grid which requires designing and applicant of power electronic converters.

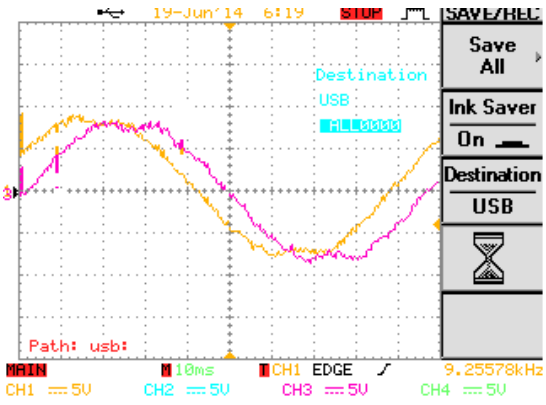

(a)

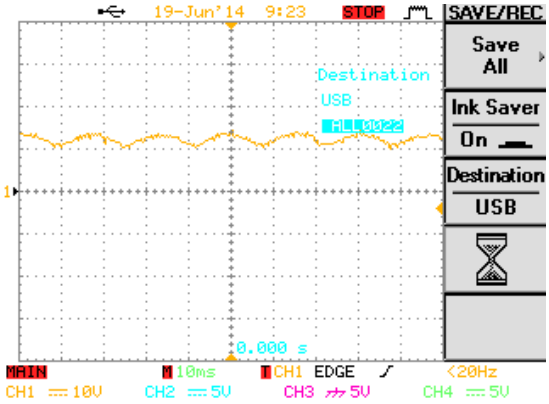

(b)

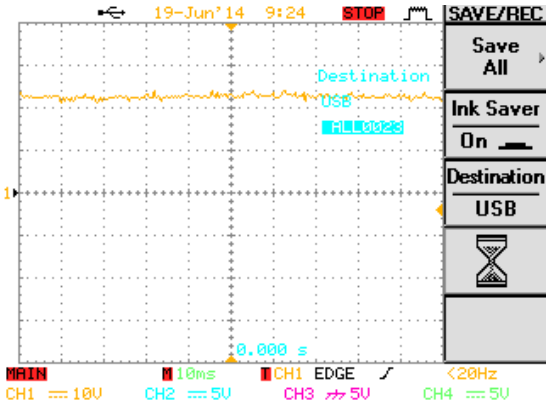

(c)

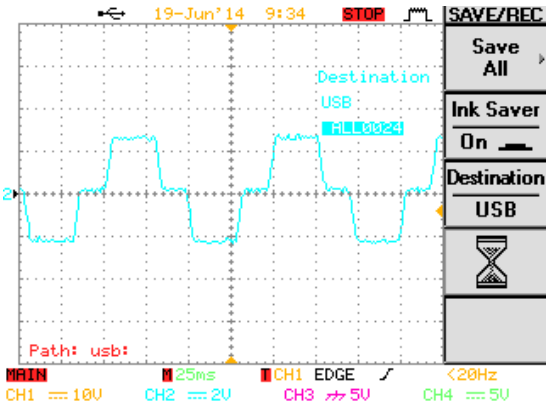

(d)

Fig. 7. Experimental test, (a) similar phase voltages of two winding sets, (b) the rectified voltage of one winding sets, (c) load DC output voltage. (10*10 V/DIV), (d) current of phase A (2*0.8 A/DIV).

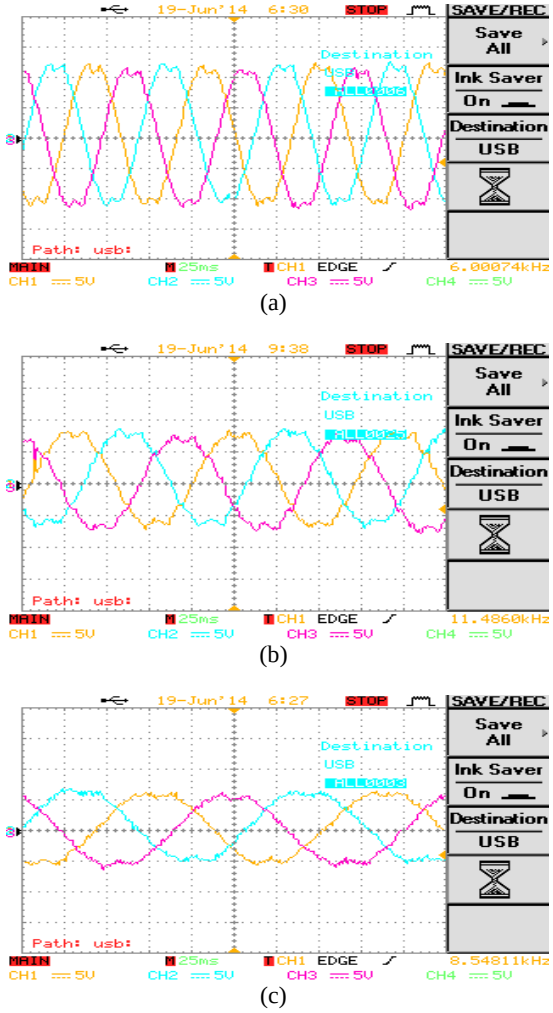

Fig. 8. Experimental test: three phase voltage of one winding sets in rotor speeds, (a) 300 R.P.M, (b) 210 R.P.M, (c) 154 R.P.M (10*10 V/DIV).

5. CONCLUSION

This research work presented performance evaluation of a dual-star permanent magnetic synchronous generator, which is suitable for low speed applications such as wind turbines. The dynamic modeling and experimental test of the dual-star PMSG and conventional PMSG carried out. The simulation and experimental test results on a system realized in the laboratory proved that the DC link current and voltage ripple has been reduced in the comparison of single winding PMSG. Besides, the experimental results proved the linear function of the speed and generator output voltage. The experimental results have an acceptable agreement with the corresponding simulation results. All these characteristics of the suggested topology make it suitable for wind turbine application in view of power electronic converter design.

ACKNOWLEDGMENT

This research has been supported by Azarbaijan Shahid Madani University

CONFLICT OF INTEREST

No conflict of interest was declared by the authors.

REFERENCES

1. S. M. Dehghan, M. Mohamadian, and A. Y. Varjani, A New Variable-Speed Wind Energy Conversion System Using Permanent-Magnet Synchronous Generator and Z-Source Inverter, IEEE Transactions on Energy Conversion, 24: 714-724 (2009).

2. S. Zhang, K.-J. Tseng, D. M. Vilathgamuwa, T. D. Nguyen, and X.-Y. Wang, Design of a Robust Grid Interface System for PMSG-Based Wind Turbine Generators, IEEE Transactions on Industrial Electronics, 58:316-328 (2011).

3. C. H. Ng, M. A. Parker, L. Ran, P. J. Tavner, J. R. Bumby, and E. Spooner, A Multilevel Modular Converter for a Large, Light Weight Wind Turbine Generator, IEEE Transactions on Power Electronics, 2:31062-1074 (2008).

4. Z. Chen, J. M. Guerrero, and F. Blaabjerg, A review of the state of the art of power electronics for wind turbines, IEEE Transactions on Power Electronics, 24:1859-1875 (2009).

5. J. M. Carrasco, L. G. Franquelo, J. T. Bialasiewicz, E. Galvan, R. C. P. Guisado, A. M. Prats, J. I. Leon, and N. Moreno-Alfonso, Powerelectronic systems for the grid integration of renewable energy sources: A survey, IEEE Transactions on Industrial Electronics, 53:1002-1016 (2006).

6. H. Polinder, F. F. A. Van de Pijl, G.-J. de Vilder, and P. J. Tavner, Comparison of Direct Drive and Geared Generator Concepts for Wind Turbines, IEEE Transactions on Energy Conversion, 21:725-733 (2006).

7. M. Chinchilla, S. Arnaltes, and J. C. Burgos, Control of Permanent-Magnet Generators Applied to Variable-Speed Wind-Energy Systems Connected to the Grid, IEEE Transactions on Energy Conversion, 21: 130-135 (2006).

8. A.D. Hansen and G. Michalke, Multi-pole Permanent Magnet Synchronous Generator Wind Turbines' Grid Support Capability in Uninterrupted Operation During Grid Faults, IET Renewable Power Generation, 3: 333-348 (2009).

9. Hua Geng, Dewei Xu, Stability Analysis and Improvements for Variable-Speed Multi pole Permanent Magnet Synchronous Generator-Based Wind Energy Conversion System, IEEE Transactions on Sustainable Energy,2: 459-467 (2011).

10. Kyoung-Jin Ko, Seok-Myeong Jang, Ji-Hoon Park, Han-Wook Cho, Dae-Joon You, Electromagnetic Performance Analysis of Wind Power Generator With Outer Permanent Magnet Rotor Based on Turbine Characteristics Variation Over Nominal Wind Speed, IEEE Transactions on Magnetics, 47: 3292-3295 (2011).

11. Wei Qiao ; Liyan Qu ; Harley, R.G., Control of IPM Synchronous Generator for Maximum Wind Power Generation Considering Magnetic Saturation, 45: 1095-1105 (2009).

12. Mauro Andriollo, Giulio Bettanini, Giovanni Martinelli, Augusto Morini, Andrea Tortella, Analysis of Double Star Permanent Magnetic Synchronous Generator by a General Decoupled d-q model, IEEE Transaction on Industry Applications, 45 (4):1416-1424 (2009).

13. Samuli Kallio, Jussi Karttunen, Pasi Peltoniemi, Pertti Silventoinen, Olli Pyrhönen, Determination of the inductance parameters for the decoupled d–q model of double-star permanent-magnet synchronous machines, IET Electric Power Applications, 8(2):39-49 (2014).

14. Shinji Kato, Yoshitaka Inui, Masakazu Michihira, Akira Tsuyoshi, A Low-Cost Wind Generator System with a Permanent Magnet Synchronous Generator and Diode Rectifiers, IEEE International Symposium on Industrial Electronics (ISIE), 1063 – 1068 (2011).

15. Shinji Kato, Masakazu Michihira, A Comparative Study on Power Generation Characteristics of Permanent Magnet Synchronous Generators, International Power Electronic Conference, 1499-1505 (2010).